J Toxicol Pathol 2019; 32: 79–89

Original Article

Dimethyl fumarate ameliorates cisplatin-induced renal tubulointerstitial lesions

Ayaka Sasaki[1], Natsumi Koike[1], Tomoaki Murakami[1], and Kazuhiko Suzuki[1]*

[1] Laboratory of Veterinary Toxicology, Cooperative Department of Veterinary Medicine, Tokyo University of Agriculture and Technology, 3-5-8 Saiwai-cho, Fuchu, Tokyo 183-8509, Japan

Abstract: Dimethyl fumarate (DMF) has an antioxidant effect by activating the nuclear factor erythroid 2-related transcription factor 2 (Nrf2). Cisplatin (CIS) has nephrotoxicity as a frequently associated side effect that is mainly mediated by oxidative stress. In this study, we investigated whether the DMF-mediated antioxidative mechanism activated by Nrf2 can ameliorate CIS-induced renal tubulointerstitial lesions in rats. In Experiments 1 and 2, 25 five-week-old male Wistar rats were divided into five groups: control, CIS, and 3 CIS+DMF groups (300, 1,500, and 7,500 ppm in Experiment 1; 2,000, 4,000, and 6,000 ppm in Experiment 2). Rats were fed their respective DMF-containing diet for 5 weeks. CIS was injected 1 week after starting DMF administration, and the same volume of saline was injected into the control group. CIS-induced severe tubular injury, such as necrosis and degeneration in the outer segment of the outer medulla, was inhibited in the 7,500 ppm DMF group and ameliorated in all DMF groups in Experiment 2. Increased interstitial mononuclear cell infiltration and increased Sirius red-positive areas were also observed in CIS-administered groups, and these increases tended to be dose-dependently inhibited by DMF co-administration in Experiments 1 and 2. The numbers of α-smooth muscle actin (SMA)-positive myofibroblasts, CD68-positive macrophages, and CD3-positive lymphocytes observed in the peritubular area also increased with CIS administration, and these increases were dose-dependently inhibited by DMF co-administration. Moreover, renal cortical mRNA expression of Nrf2-related genes such as NQO1 increased in DMF groups. This investigation showed that DMF ameliorates CIS-induced renal tubular injury via NQO1-mediated antioxidant mechanisms and reduces the consequent tubulointerstitial fibrosis. (DOI: 10.1293/tox.2018-0049; J Toxicol Pathol 2019; 32: 79–89)

Key words: dimethyl fumarate, cisplatin, renal injury, antioxidant

Introduction

Chronic kidney disease (CKD) is a common pathological condition that includes various kidney diseases, such as glomerulonephritis, vascular injury, and tubulointerstitial nephritis, and it is a problem worldwide. There is a high prevalence of CKD in humans. In veterinary medicine, CKD is widely found in dogs and cats, and especially in aging cats, its prevalence is estimated to be ≥30–40%[1]. Thus, further elucidation of CKD and its manifestation is required in both the medical and veterinary fields. Renal tubular damage following interstitial fibrosis is a common finding in CKD, and its development rate is closely related to renal dysfunction. Fibrosis is an overreaction of tissue repair, and its mechanism is considerably intricate and involves many factors including myofibroblasts, macrophages, and cytokines such as TGF-β. Several experimental models have been used to study the mechanisms of interstitial fibrosis[2–8], and among the chemical-induced models is the cisplatin (CIS)-induced model. CIS is a useful anti-cancer agent but it has several side effects, such as nephrotoxicity, and the CIS-induced model is widely used to investigate the mechanism of tubulointerstitial fibrosis and to evaluate therapeutic strategies against nephrotoxicity. The pathogenesis of CIS-induced nephrotoxicity includes apoptosis, oxidative stress, and DNA damage, and because oxidative stress can induced apoptosis and DNA damage, it is an important factor for CIS-induced nephrotoxicity[9–12].

Dimethyl fumarate (DMF) is a recently approved therapeutic agent for multiple sclerosis and psoriasis. DMF has a broad spectrum of action, which includes such things as switching the immune response from Th1-dependent to Th2-dependent[13], increasing in anti-inflammatory cytokine production[14], and induction of an antioxidant effect through activation of nuclear factor erythroid 2-related transcription factor 2 (Nrf2)[15]. Nrf2 is a heterodimer of p45 and a member of the Maf family of proteins, and it stimulates expression of antioxidant-related genes such as heme oxygenase-1 (HO-1), NAD(P)H quinone oxidoreductase 1 (NQO1), and glutathione S-transferase mu 1 (Gstm1). These antioxidant-related genes, especially HO-1, are protective against CKD

Received: 28 September 2018, Accepted: 19 December 2018
Published online in J-STAGE: 19 January 2019
*Corresponding author: K Suzuki (e-mail: kzsuzuki@cc.tuat.ac.jp)

and acute kidney injury (AKI)[16–18]. Previous studies suggested that DMF attenuates renal fibrosis in TGF-β-treated rat mesangial cells (RMCs), renal fibroblasts both *in vitro* and *in vivo*[19], and CD68+ renal macrophage infiltration[20] via an Nrf2-mediated mechanism. Additionally, DMF was recently shown to ameliorate lung fibrosis in a bleomycin-induced lung fibrosis model, and this mechanism is speculated to occur via antioxidants and reduced pro-inflammatory and pro-fibrotic gene expression to prevent pathological collagen deposition[21]. Based on these findings, this investigation aimed to determine whether DMF-mediated antioxidative mechanisms activated by Nrf2 can ameliorate CIS-induced renal tubular injury and subsequent tubulointerstitial fibrosis in rats.

Materials and Methods

Chemicals

CIS solution (0.5 mg/mL) was purchased from Nichiiko Pharmaceutical Co., Ltd. (Toyama, Japan), and DMF was purchased from Wako Pure Chemical Industries Co., Ltd. (Osaka, Japan). All other chemicals were obtained commercially.

Animals and experimental design

All efforts were made to minimize the number of animals used and any suffering they might experience. All procedures in this study were conducted in accordance with the Guide for Animal Experimentation of Tokyo University of Agriculture and Technology.

Five-week-old male Wistar rats were purchased from SLC Japan (Shizuoka, Japan). Because previous toxicology tests revealed that there were no sex differences in CIS-induced nephrotoxicity, based on similar previously published studies, we used male rats in this experiment. Rats were housed in temperature-controlled cages with a 12-h light/dark cycle and were allowed ad libitum access to tap water and a powdered CRF-1 basal diet (Oriental Yeast Co., Ltd., Tokyo, Japan). Animals were acclimatized for 1 week and divided into five group: control (n=5), CIS (n=5), CIS + DMF 300 ppm (n=5), CIS + DMF 1,500 ppm (n=5), and CIS + DMF 7,500 ppm (n=5). The control group was fed a normal diet. The middle DMF doses were set based on the results of preliminary experiments that were performed by Zhang *et al.*[22]. When we decided upon these doses, we expected that the renal lesions would be ameliorated by the 300 and 1,500 ppm doses and inhibited by the 7,500 ppm dose. Rats were fed their respective DMF-containing diet for 5 weeks. At 1 week after the start of DMF administration, a single dose of intraperitoneal CIS (6 mg/kg; i.e., 12 mL/kg) was administrated to all CIS groups. The control group was administered saline intraperitoneally at the same volume. During the experimental period, the general conditions of the animals were observed, food and water consumption were measured daily, and body weight was measured once every 2 days. Four weeks after CIS administration, all rats were sacrificed by exsanguination from the abdominal aorta under isoflurane anesthesia. The left and right kidneys were excised and weighed, and the relative weight was calculated as a percent of the terminal body weight.

When the histopathological changes were evaluated, the inhibitory effect of 1,500 ppm DMF was milder than expected. Therefore, we redesigned the experiment. In Experiment 2, the animals were also divided into five group: control (n=5), CIS (n=5), CIS + DMF 2,000 ppm (n=5), CIS + DMF 4,000 ppm (n=5), and CIS + DMF 6,000 ppm (n=5). The other procedures were the same as for Experiment 1.

For histopathology and immunohistochemistry, the kidney obtained from each rat was fixed using periodate-lysine-paraformaldehyde (PLP)–acetone, methyl benzoate, and xylene (AMeX)[23]. Briefly, specimens were immersed in the PLP fixative (containing 4% paraformaldehyde) for 7 h at 4°C and then washed with phosphate-buffered saline (PBS; 0.01 M, pH 7.4) for 2 h at 4°C. Then, the tissues were dehydrated in acetone overnight at 4°C and twice for 1 h each at room temperature, cleared twice in methyl benzoate for 30 min followed by xylene twice for 30 min, soaked three times in paraffin for 40 min each at 60°C, and embedded in paraffin. The paraffin blocks prepared using the PLP-AMeX method were stored at 4°C. The kidney tissue for PCR was collected by cutting the renal cortex into small pieces, freezing it, and storing it at −80°C.

Blood biochemistry

Blood urea nitrogen (BUN) and serum creatinine (Cre) were measured in serum samples obtained from each rat at the end of the experimental period. The measurements were performed by a commercial inspection agency.

Histopathology

Paraffin sections (2 μm) were stained using hematoxylin and eosin (HE) and Sirius red for histopathological examination. For quantification of the Sirius red-positive area, five fields were selected at 100× magnification from the outer segment of the outer medulla in the right and left kidneys and analyzed using Image J software (National Institutes of Health, Bethesda, MD, USA).

Immunohistochemistry

For immunohistochemistry, the 2-μm sections were deparaffinized and soaked in methanol containing 0.3% hydrogen peroxide for 30 min to block endogenous peroxidase activity. The sections were then treated with 10% normal goat serum for 30 min to block nonspecific reactions. Anti-α-smooth muscle actin (α-SMA) antibody (mouse polyclonal, Dako, Denmark; diluted ×200), anti-CD68 antibody (mouse polyclonal, BMA Biomedicals, Switzerland; diluted ×100), anti-CD3 antibody (rabbit polyclonal, Abcam Plc., UK; diluted ×100), and anti-Nrf2 antibody (rabbit polyclonal, Abcam Plc., UK; diluted ×100) were used as the primary antibodies and incubated overnight at 4°C. Each section was then incubated with EnVision solution (Dako, Denmark) against mouse or rabbit immunoglobulin (Ig) G for 30 min at room temperature. Antibody-binding was

Table 1. Equences of Primer Used for Real-time PCR

Target	Forward	Reverse
Nrf2	ACCTGTGAGTCCTGGTCATCAAA	GAGCCTCTAATCGGCTTGAATG
HO1	GGTGATGGCCTCCTTGTACC	GTGGGGCATAGACTGGGTTC
NQO1	GTTTGCCTGGCTTGCTTTCA	ACAGCCGTGGCAGAACTATC
G6PD	CCTACCATCTGGTGGCTGTT	GAAGGGCTCACTCTGTTTGC
ME1	CGACCAGCAAAGCTGAGTGTT	CTGCCGCTGGCAAAGATC
TNFα	TGCCTCAGCCTCTTCTCATTC	GCTCCTCTGCTTGGTGGTTT
IL4	ACCTTGCTGTCACCCTGTTCT	AGCTCGTTCTCCGTGGTGT
IL6	CCCACCAGGAACGAAAGTCA	CTTGCGGAGAGAAACTTCATAGC
IL10	CTGTCATCGATTTCTCCCCTGT	CAGTAGATGCCGGGTGGTTC
CD206	ACTGCGTGGTGATGAAAGG	TAACCCAGTGGTTGCTCACA
HPRT-1	GCCGACCGGTTCTGTCAT	TCATAACCTGGTTCATCATCACTAATC

visualized using 3,3-diaminobenzidine (DAB) chromogen and counterstained with Mayer's hematoxylin. The number of each type of antibody-positive cells was counted in 50 fields per section at 400× magnification in the outer segment of the outer medulla in the right and left kidneys, and an average number per field was calculated.

Real-time revere transcription polymerase chain reaction (real-time RT-PCR) analysis

Total RNA was extracted from the renal cortical tissue of each rat using an RNeasy Mini Kit (QIAGEN, The Netherlands). The concentration of total RNA samples was measured using Gen5 2.0 (BioTek Instruments, Inc., Winooski, VT, USA). Then, cDNA was prepared from 500 ng of total RNA using PrimeScript RT Master Mix (Takara Bio Inc, Shiga, Japan) in a LifeECO Thermal Cycler (Bioer Technology Co., Ltd, Hangzhou, China) at 37°C for 15 min and 85°C for 5 s. Real-time polymerase chain reaction (PCR) was performed using SYBR Premix Ex Taq II (Takara Bio Inc, Shiga, Japan) in a Thermal Cycler Dice Real Time System II (Takara Bio Inc, Shiga, Japan) (95°C for 30 s; 40 cycles of 95°C for 5 s and 60°C for 30 s; 95°C for 15 s; 60°C for 30 s; and 95°C for 15 s). Six targets for antioxidant-related factors (Nrf2, heme oxygenase (HO)-1, NAD(P)H quinone dehydrogenase (NQO) 1, glucose-6-phosphate dehydrogenase (G6PD), malic enzyme (Me) 1) and five targets for inflammation-related factors (tumor necrosis factor (TNF)-α, interleukin (IL)-4, IL-6, IL-10, CD206) were analyzed. Primer sequences are presented in Table 1. The relative differences in gene expression were calculated using cycle time (Ct) values that were normalized to those of hypoxanthine phosphoribosyltransferase (HPRT)-1, an endogenous control in the same sample, and then the expression level relative to controls was obtained using the $2^{-\Delta\Delta C_T}$ method[24].

Statistical analysis

All obtained data were expressed as the mean ± SD. The statistical analysis was performed using a one-way analysis of variance (ANOVA) followed by Tukey's post-hoc test for multiple comparisons. $P<0.05$ was considered significant.

Results

Experiment 1

Body and kidney weight, and daily food and chemical intake: The data are shown in Table 2. Final body weight did not differ between the control and CIS groups, but it decreased in a dose-dependent manner in the DMF groups. The absolute kidney weights in the CIS and DMF 7,500 ppm groups were also similar to that in the control group, and those of the DMF 300 and DMF 1,500 ppm groups were significantly increased. Additionally, the relative kidney weight in the CIS group was similar to that in the control group, but it was significantly increased in all DMF groups. The average daily food intake significantly decreased in the DMF 7,500 ppm group. The average DMF intake in the DMF groups was calculated from the amount of daily food intake.

Blood biochemistry: BUN tended to be increased by CIS administration, and Cre was significantly higher in the CIS group compared with the control group. BUN levels were decreased by a higher dose of DMF compared with the CIS group (Fig. 1A). However, Cre was dose-dependently decreased in the DMF 1,500 and DMF 7,500 ppm groups compared with the CIS group (Fig. 1C).

Histopathology: CIS induced severe necrosis, degeneration, and luminal dilation and moderate urinary casts, especially in the proximal tubules in the outer segment of the outer medulla (Fig. 2B, F). These tubular injuries (necrosis and degeneration of tubular epithelial cells, luminal dilation of renal tubules, and urinary casts) were recovered to the control level only in the 7,500 ppm DMF group (Fig. 2I, M). In addition to tubular lesions, mononuclear cell infiltration was observed in the tubulointerstitium and around arterioles and peritubular fibrosis in CIS-treated groups. Mononuclear cell infiltration tended to decrease in a dose-dependent manner in the 300 ppm (Fig. 2G) and 1,500 ppm (Fig. 2M) DMF groups, and it was hardly ever observed in the 7,500 ppm DMF group.

When the degree of peritubular fibrosis was evaluated using Sirius red stain, the positive area was found to be significantly increased in the CIS group compared with the control group but was found to be decreased in the DMF 300 and 1,500 ppm groups and to have recovered to control

Table 2. Body and Kidney Weight, Daily Food and DMF Intake

	Exp. 1				
	Control	CIS	CIS + DMF 300 ppm	CIS + DMF 1,500 ppm	CIS + DMF 7,500 ppm
Final body weight (g)	268.5 ± 7.62	242.55 ± 8.96	235.02 ± 23.08	226.52 ± 14.23*	175.76 ± 17.52$^{**,++}$
Kidney Absolute (g)	1.59 ± 0.12	1.56 ± 0.11	1.90 ± 0.21$^{*,++}$	1.97 ± 0.18$^{**,++}$	1.46 ± 0.11
Relative (g/100g BW)	0.59 ± 0.027	0.65 ± 0.064	0.81 ± 0.12$^{**,++}$	0.87 ± 0.069$^{**,++}$	0.83 ± 0.042$^{**,++}$
Average food intake (g/day)	14.81 ± 1.71	14.25 ± 1.18	13.84 ± 1.61	13.07 ± 1.74	10.19 ± 0.89$^{**,++}$
Average DMF intake (mg/kg/day)	–	–	17.6 ± 2.02	86.35 ± 11.69	431.47 ± 42.34
	Exp. 2				
	Control	CIS	CIS + DMF 2,000 ppm	CIS + DMF 4,000 ppm	CIS + DMF 6,000 ppm
Final body weight (g)	259.75 ± 11.54	236.45 ± 9.49	199.66 ± 16.7$^{**,+}$	191.78 ± 24.15$^{**,++}$	168.36 ± 28.29$^{**,++}$
Kidney Absolute (g)	1.51 ± 0.055	1.47 ± 0.13	1.85 ± 0.32	1.62 ± 0.18	1.53 ± 0.37
Relative (g/100g BW)	0.58 ± 0.018	0.61 ± 0.044	0.92 ± 0.09$^{**,++}$	0.85 ± 0.042$^{**,++}$	0.90 ± 0.047$^{**,++}$
Average food intake (g/day)	14.21 ± 1.65	13.87 ± 1.22	12.92 ± 4.42	11.23 ± 3.19$^{**,++}$	8.65 ± 2.07$^{**,++}$
Average DMF intake (mg/kg/day)	–	–	129.2 ± 47.22	233.91 ± 71.08	339.21 ± 86.61

Data are expressed as the mean ± SD. $^{*}P<0.05$ compared with the control group. $^{**}P<0.01$ compared with the control group. $^{+}P<0.05$ compared with the CIS group. $^{++}P<0.01$ compared with the CIS group.

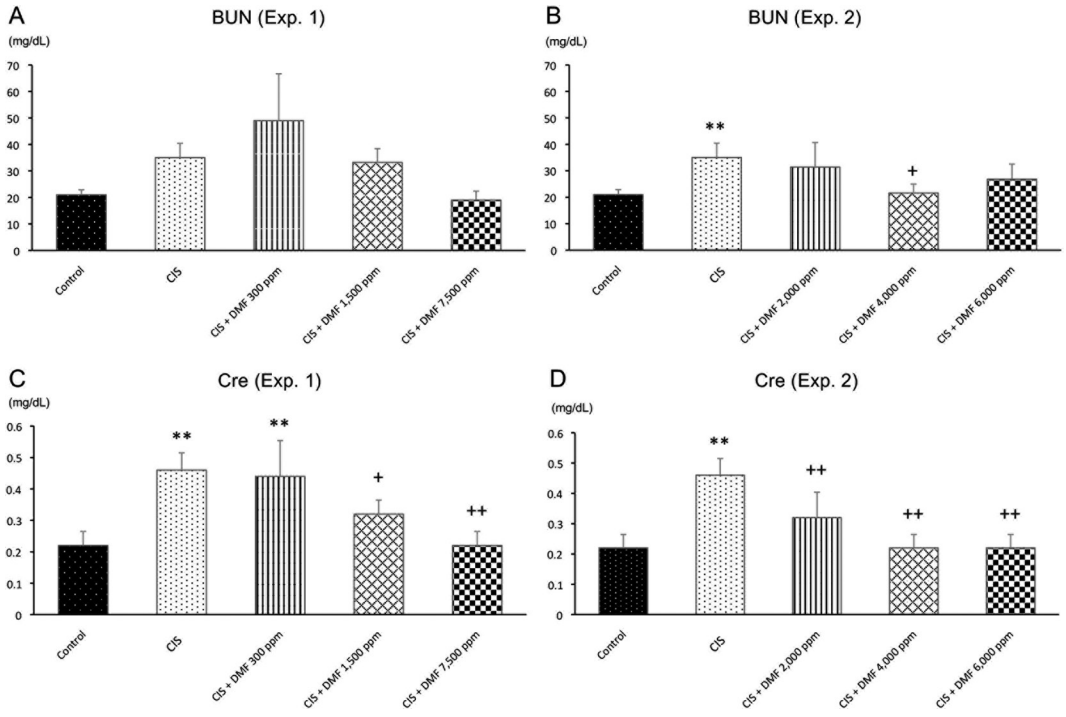

Fig. 1. Blood biochemistry: serum BUN (A and B) and Cre (C and D) in Experiment 1 (A and C) and Experiment 2 (B and D). Data are presented as the mean ± SD. $^{**}P<0.01$ compared with the control group. $^{+}P<0.05$ compared with the CIS group. $^{++}P<0.01$ compared with the CIS group.

levels in the DMF 7,500 ppm group (Fig. 3A–E, I).

Immunohistochemistry: Compared with the control group, the numbers of α-SMA-, CD68-, and CD3-positive cells per field were significantly increased in the CIS group. Among the infiltrating cells observed in the tubulointerstitium and around arterioles, CD68-positive cells were predominant rather than CD3-positive cells. α-SMA-positive cells were particularly observed around the dilated tubules. The numbers of α-SMA- and CD68-positive cells were significantly and dose-dependently decreased with DMF 1,500 or 7,500 ppm compared with the CIS group (Fig. 4A, C). Additionally, the number of CD3-positive cells was significantly and dose-dependently decreased in all DMF groups compared with the CIS group (Fig. 4E).

Nrf2-positive cells were mainly located in the tubular epithelial cells. The number of Nrf2-positive cells was significantly increased in the DMF 7,500 ppm group, but there were no significant differences among any of the other treated groups (Fig. 5A).

Changes of mRNA expression: The data are shown in Table 3. Among antioxidant-relative genes, NQO1 mRNA expression was significantly and dose-dependently in-

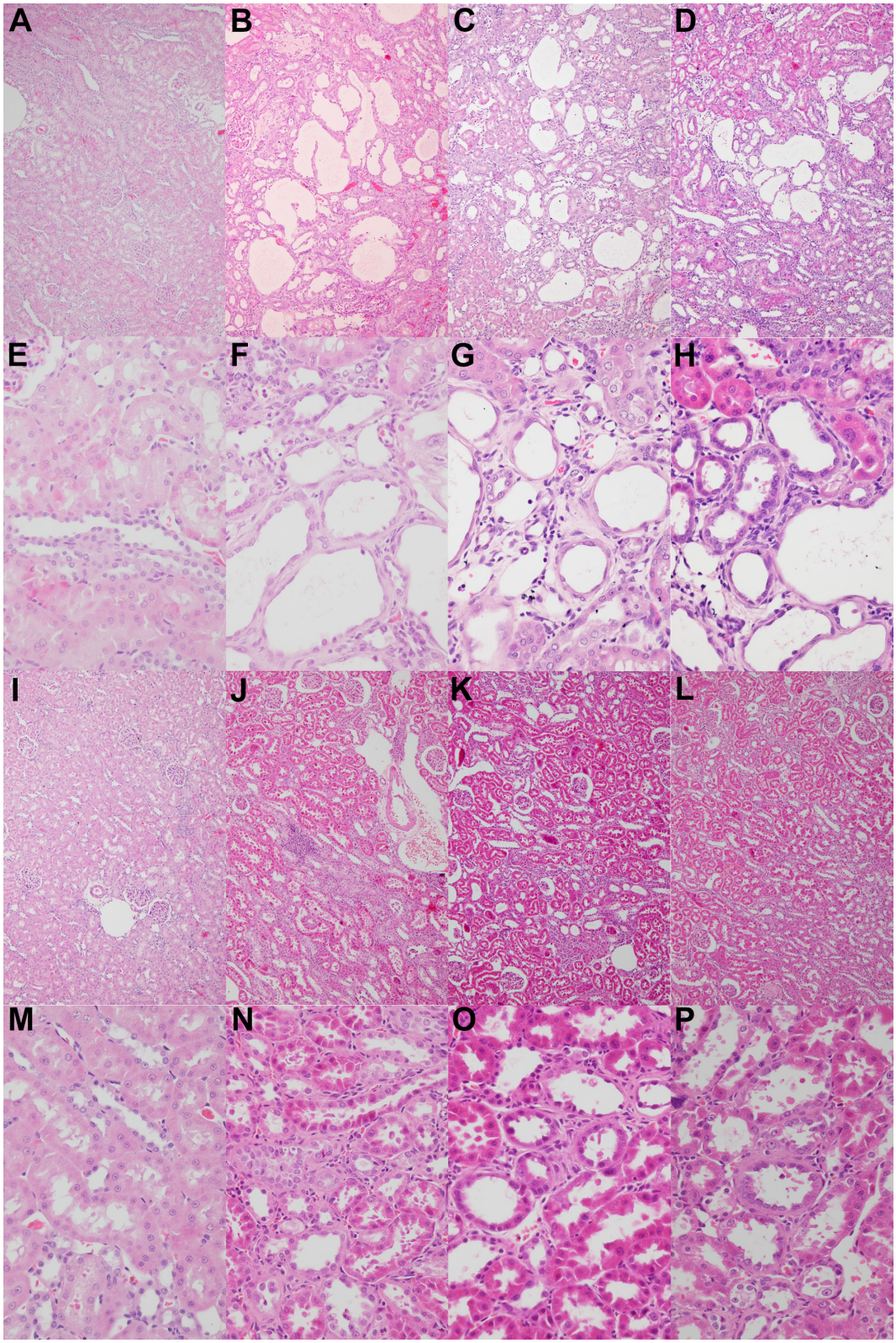

Fig. 2. Histopathological changes. There was no change in the control group (A and E). In Experiment 1, tubular lesions such as necrosis, degeneration, and luminal dilation; mononuclear cell infiltration; and peritubular fibrosis were prominent in the CIS group (B and F). These histological changes were ameliorated by 300 ppm (C and G) and 1,500 ppm (D and H) DMF and recovered to the control level by 7,500 ppm DMF (I and M). Additionally, in Experiment 2, these changes were dose-dependently ameliorated in the 2,000 ppm (J and N), 4,000 ppm (K and O), and 6,000 ppm (L and P) DMF groups. Hematoxylin and eosin staining. Magnification: ×100 (A–D and I–L) or ×400 (E–H and M–P).

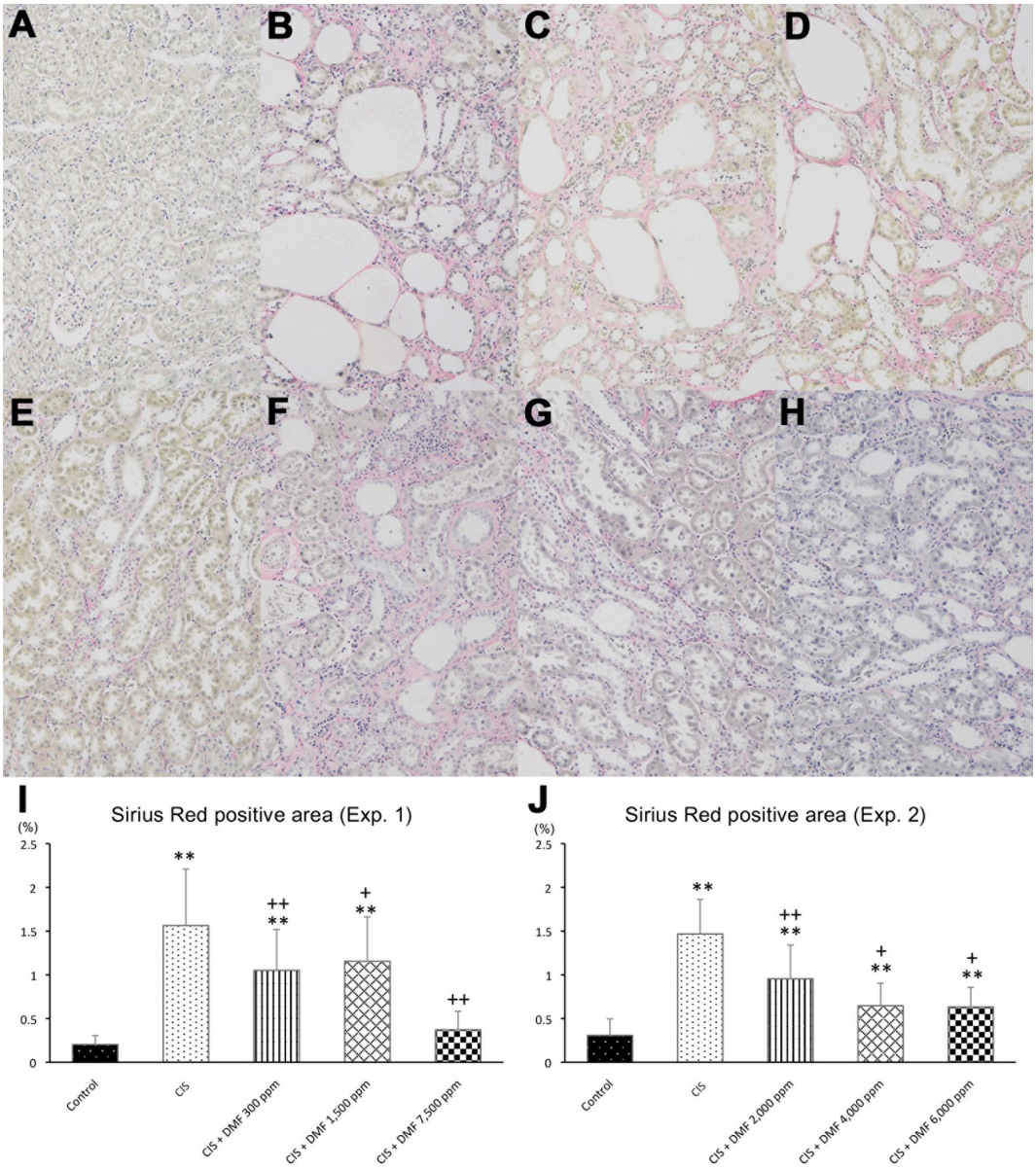

Fig. 3. Peritubular fibrosis was not observed in the control group (A), but it was prominent in the CIS group (B). In Experiment 1, fibrosis was ameliorated by 300 ppm (C) and 1,500 ppm (D) of DMF, and it recovered to control levels with 7,500 ppm of DMF (E and I). Additionally, in Experiment 2, these changes were dose-dependently ameliorated in all DMF groups (F–H, J). Magnification: ×100 (A–H). Data are expressed as the mean ± SD. **$P<0.01$ compared with the control group. $^{+}P<0.05$ compared with the CIS group. $^{++}P<0.01$ compared with the CIS group.

creased with DMF doses above DMF 1,500 ppm, but HO-1 mRNA expression showed no significant differences among the groups. For other genes that are also controlled by Nrf2 activation, G6PD mRNA expression was significantly increased in the 7,500 ppm DMF group compared with the control group. Me1 mRNA expression significantly decreased in the CIS group and recovered to control levels in the 7,500 ppm DMF group. Cytokine mRNA expression tended to increase in response to CIS administration, and this increase was suppressed by DMF. The same tendency was observed for CD206 mRNA expression. For Nrf2 mRNA expression, no significant differences were observed among the groups.

Experiment 2

When the histopathological changes were evaluated, the inhibitory effect of 1,500 ppm DMF was milder than expected. Therefore, we redesigned the experimental doses to fall between 1,500 and 7,500 ppm (i.e., 2,000 ppm, 4,000, ppm, and 6,000 ppm) in Experiment 2.

Body and kidney weight, and daily food and chemical intake: The data are shown in Table 2. Similar to Experi-

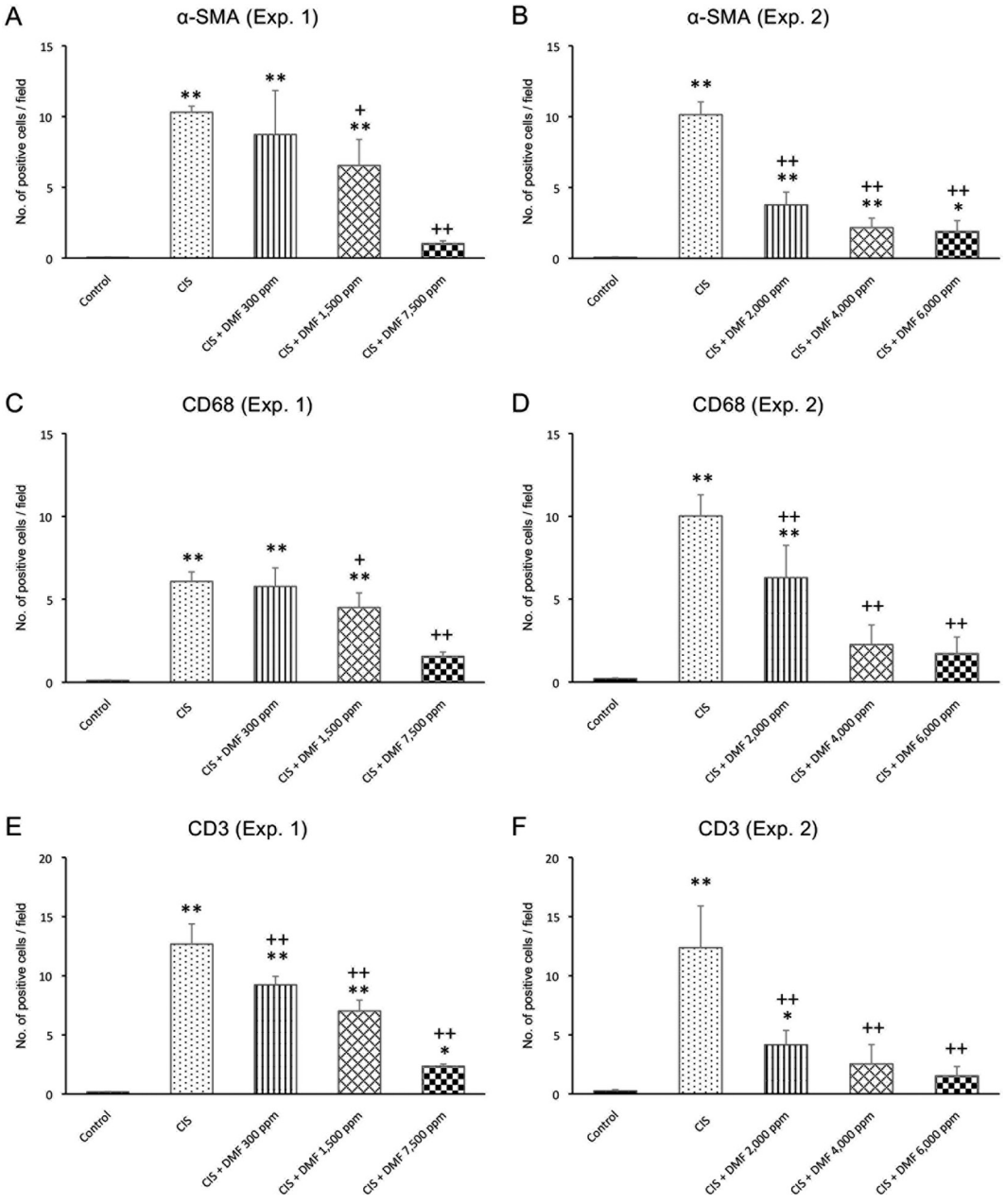

Fig. 4. The numbers of α-SMA- (A and B), CD68- (C and D), and CD3-positive cells (E and F) in Experiment 1 (A, C, and E) and Experiment 2 (B, D, and F). Data are expressed as the mean ± SD. **P*<0.05 compared with the control group. ***P*<0.01 compared with the control group. ^{+}P<0.05 compared with the CIS group. ^{++}P<0.01 compared with the CIS group.

ment 1, final body weight was not different between the control and CIS groups, but it was dose-dependently decreased in all DMF groups. The absolute kidney weights in the CIS and DMF 6,000 ppm groups were similar to that in control group, but slight, but not significant, increases were observed in the DMF 2,000 and 4,000 ppm groups. Additionally, in Experiment 2, the relative kidney weight in the CIS group was similar to that in the control group, but it was significantly increased in all DMF groups compared with the control group. The average daily food intake significantly decreased in the DMF 6,000 ppm group.

Blood biochemistry: BUN and Cre were significantly higher in the CIS group compared with the control group. BUN had a tendency to be decreased by DMF compared with the CIS group (Fig. 1B). Cre was significantly and dose-dependently decreased in all DMF groups compared with the CIS group (Fig. 1D).

Histopathology: CIS induced severe necrosis, degeneration, and luminal dilation and moderate urinary casts, especially in the proximal tubules in the outer segment of the outer medulla. These tubular injuries were ameliorated in all DMF groups (Fig. 2J–L, N–P). Mononuclear cell infil-

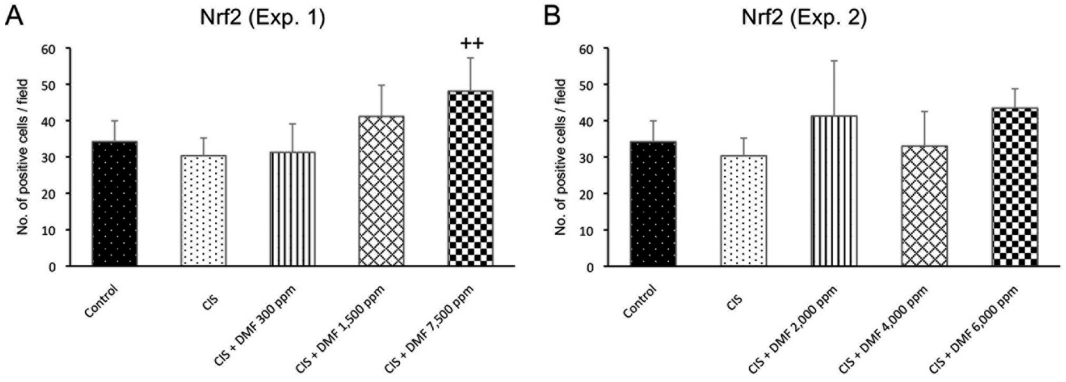

Fig. 5. The numbers of Nrf2-positive cells in Experiment 1 (A) and Experiment 2 (B). Data are expressed as the mean ± SD. $^{++}P<0.01$ compared with the CIS group.

Table 3. The Relative Expression of Several Genes Analyzed by Real-time RT-PCR

Exp. 1					
	Control	CIS	CIS + DMF 300 ppm	CIS + DMF 1,500 ppm	CIS + DMF 7,500 ppm
Nrf2	1.00 ± 0.14	1.20 ± 0.07	1.32 ± 0.23	1.25 ± 0.45	1.04 ± 0.38
HO-1	1.00 ± 0.64	1.21 ± 0.50	1.07 ± 0.15	1.19 ± 0.36	1.65 ± 0.51
NQO1	1.00 ± 0.21	1.20 ± 0.44	1.81 ± 0.50	2.8 ± 0.88**,+	4.63 ± 1.08**,++
G6PD	1.00 ± 0.13	1.24 ± 0.27	1.63 ± 0.40	1.73 ± 0.48	1.89 ± 0.72*
Me1	1.00 ± 0.24	0.53 ± 0.21**	0.43 ± 0.09**	0.56 ± 0.13*	1.03 ± 0.22++
TNF-α	1.00 ± 0.55	2.70 ± 1.05*	2.14 ± 0.76	1.98 ± 0.64	1.08 ± 0.57+
IL-6	1.00 ± 1.26	0.94 ± 1.14	2.32 ± 1.02	2.15 ± 2.32	0.46 ± 0.33
IL-4	1.00 ± 1.93	6.70 ± 13.15	15.99 ± 23.74	1.77 ± 3.88	1.98 ± 4.16
IL-10	1.00 ± 1.09	3.14 ± 2.50	3.19 ± 3.20	1.46 ± 1.13	1.25 ± 2.13
CD206	1.00 ± 0.57	4.86 ± 1.48	6.91 ± 5.47*	5.01 ± 1.28	2.48 ± 1.99
Exp. 2					
	Control	CIS	CIS + DMF 2,000 ppm	CIS + DMF 4,000 ppm	CIS + DMF 6,000 ppm
Nrf2	1.00 ± 0.08	1.29 ± 0.14	1.26 ± 0.14	0.99 ± 0.18	0.98 ± 0.10
HO-1	1.00 ± 0.37	2.04 ± 0.60	1.43 ± 0.65	1.67 ± 0.9	1.56 ± 0.64
NQO1	1.00 ± 0.57	1.36 ± 0.40	1.79 ± 0.56	7.65 ± 1.50**,++	8.74 ± 3.19**,++
G6PD	1.00 ± 0.22	1.54 ± 0.15	1.23 ± 0.27	1.53 ± 0.21	1.50 ± 0.53
Me1	1.00 ± 0.35	0.59 ± 0.37	0.30 ± 0.05**	0.61 ± 0.11	0.50 ± 0.11
TNF-α	1.00 ± 0.73	0.42 ± 0.21	0.89 ± 0.24	1.04 ± 0.41	0.75 ± 0.19
IL-6	1.00 ± 1.08	1.07 ± 1.13	0.19 ± 0.25	0.13 ± 0.09	0.03 ± 0.02
IL-4	1.00 ± 2.01	1.46 ± 2.36	0.14 ± 0.25	0.02 ± 0.03	0.03 ± 0.05
IL-10	1.00 ± 0.85	4.64 ± 4.36	1.95 ± 1.65	1.12 ± 0.74	1.14 ± 1.07
CD206	1.00 ± 0.56	6.55 ± 1.94**	4.95 ± 2.65*	2.91 ± 1.88+	1.56 ± 0.92++

Data are expressed as the mean ± SD. *$P<0.05$ compared with the control group. **$P<0.01$ compared with the control group. $^{+}P<0.05$ compared with the CIS group. $^{++}P<0.01$ compared with the CIS group.

tration and peritubular fibrosis were also observed in CIS-treated groups and tended to be dose-dependently inhibited by DMF co-administration.

When the degree of peritubular fibrosis was evaluated using Sirius red stain, the positive area was found to be significantly decreased in all DMF groups (Fig. 3F–H, J).

Immunohistochemistry: In Experiment 2, the numbers of α-SMA-, CD68-, and CD3-positive cells per field were significantly increased in CIS group compared with the control group. The numbers of α-SMA-, CD68-, and CD3-positive cells were significantly and dose-dependently decreased in all DMF groups compared with the CIS group (Fig. 4B, D, F). However, the number of Nrf2-positive cells showed no significant difference among the groups (Fig. 5B).

Changes of mRNA expression: The data are shown in Table 3. Among the antioxidant-relative genes, NQO1 mRNA expression was significantly and dose-dependently increased at DMF doses of 4,000 and 6,000 ppm, but HO-1 mRNA expression showed no significant differences. For other genes that are also controlled by Nrf2 activation, there were no significant changes in G6PD and Me1 mRNA expression. Cytokine mRNA expression tended to increase with CIS administration, and this increase was suppressed by DMF co-administration. The same tendency was observed for CD206 mRNA expression. For Nrf2 mRNA expression, no significant differences were observed among the groups.

Discussion

DMF was recently approved as a therapeutic agent for multiple sclerosis and psoriasis, and it is a safe medication that has no known toxicity except contact dermatitis[25]. In our study, although a reduction in body weight gain was observed in DMF-fed groups and the relative weights of the liver (data not shown) and kidney increased in both Experiments 1 and 2, there were no obvious histological changes in the major organs such as the liver, spleen, heart, and lung, and a reduction in intraperitoneal fat was observed in the DMF-fed groups (data not shown). A previous study showed that fumaric acid ester treatment may decrease visceral fat weight and ectopic fat accumulation in the liver and muscle and induce greater levels of lipolysis and incorporation of glucose into adipose tissue lipids in transgenic spontaneously hypertensive rats[26]. Based on these findings, the suppression of body weight gain observed in our study was considered to be a result of decreased food intake caused by a repelling action against DMF, as well as a decreased volume of intraperitoneal fat that may be caused by the influence of lipid metabolism, but it was not an adverse effect of DMF. Additionally, based on the decreased food intake that might be caused by the repelling action, chemical intake was unpredictably lower, especially in the higher-dose groups; this resulted in a slight difference between 1,500 ppm in Experiment 1 and 2,000 ppm in Experiment 2. However, the increasing trend in the chemical intake was not reversed, and thus, we judged that any changes examined in this study could be considered based on dose dependency.

Histopathologically, tubular injuries, such as tubular necrosis, regeneration, and luminal dilation that were induced by CIS administration, were dose-dependently ameliorated by DMF doses over 2,000 ppm. Interstitial mononuclear cell infiltration was also reduced by DMF co-administration. The evaluation of fibrosis by Sirius red staining showed that the red stained area ratio increased following CIS administration, and this increase was dose-dependently inhibited by DMF. Additionally, regarding the immunohistochemical results, the numbers of CD68-, CD3-, and α-SMA-positive cells significantly decreased in the DMF groups compared with the CIS-group. Thus, DMF may reduce the CIS-induced infiltration of mononuclear cells, including CD68-positive macrophages and CD3-positive lymphocytes, and decrease the number of α-SMA-positive myofibroblasts that are induced by CIS. Similar to our study results for CD68-positive macrophages, DMF ameliorated the infiltration of CD68-positive macrophages in a nephronophthisis model using the Lewis polycystic kidney rat[20]. CD68-positive macrophages were classified as type 1 macrophages that had proinflammatory effects, and a previous study suggested that they were involved in renal interstitial fibrosis[27]. Moreover, α-SMA-positive myofibroblasts produce extracellular matrix and play an important role in the development of fibrosis in various organs[28]. Considering the similar dose-dependent changes with respect to the decrease in fibrosis and the inhibition of increased numbers of CD68- and α-SMA-positive cells, CD206, IL-4, and IL-10 mRNA expression showed a tendency to be suppressed by DMF compared with the CIS group. CD206, IL-4, and IL-10 are classified into type 2 macrophage markers and type 2 macrophages that induce extracellular matrix production, and they are involved in fibrosis[29]. Therefore, these results suggested that DMF might ameliorate tubulointerstitial fibrosis by suppressing macrophage infiltration and the increase in myofibroblasts. However, because previous reports suggested that the regenerated proximal tubule may produce chemokines (MCP-1 and RANTES) and a fibrotic cytokine (TGF-β1) in the mercuric chloride-induced renal tubulointerstitial model, it is possible that the inhibitory effect of DMF against tubular injury decreased production of these factors, which would ameliorates the consequent macrophage infiltration and increase in myofibroblasts following tubulointerstitial fibrosis[8, 30].

In the real-time RT-PCR analysis, among the antioxidant-related genes controlled by Nrf2, NQO1 mRNA was upregulated by DMF. NQO1 mRNA expression was significantly and dose-dependently increased at 1,500 and 7,500 ppm in Experiment 1 and 4,000, and 6,000 ppm in Experiment 2. A previous study also reported the protective role of NQO1 in cisplatin-induced nephrotoxicity[31]. In contrast to NQO1, HO-1 mRNA expression did not show a significant difference among the groups. In previous studies, the protective effect of HO-1 against chronic kidney injury was observed in unilateral ureter obstruction and ischemic renal tubular necrosis models[4, 32]. Additionally, DMF induced NQO1, not HO-1, in multiple sclerosis patients[33]. Therefore, it was speculated that the oxidative stress-related factor might be different between the target organs, the target site in the kidney, and the mechanism of renal tubular injury. G6PD and Me1 are also Nrf2-regulated genes and pentose phosphate pathway-related enzymes. G6PD mRNA expression was significantly increased in the 7,500 ppm DMF group compared with the control group. Me1 mRNA expression was decreased by CIS administration, and it recovered to the control level in response to 7,500 ppm DMF. Mitsuishi et al. reported that Nrf2 directly controlled the genes of some enzymes that catalyze the oxidative and non-oxidative pathways of the pentose phosphate pathway and produce NADPH[34]. When NADPH was produced by the pentose phosphate pathway, NADPH synthesized reduced glutathione, which can decompose and remove hydrogen peroxide from oxidized glutathione and which also has antioxidant effects[35]. Therefore, it was suggested that, when DMF mediated Nrf2 stabilization, the pentose phosphate pathway was activated, and NADPH and NQO1 production, downstream of NADPH, increased. These factors then exerted antioxidative and cytoprotective effects on CIS-induced tubular injury.

For the first DMF target, Nrf2, there was no significant change in DMF groups at either the protein localization or mRNA expression level, except for a significant increase in the number of positive cells at the highest dose in Experiment 1 (7,500 ppm), which was contrary to our expectations.

This finding may be explained by the effect of DMF being stopped in the DMF-fed groups by the 5 weeks of co-administration or by an antioxidant reaction that the animal originally experienced, such as Nrf2 stabilization, which might have been experienced for 4 weeks in the CIS group. To clarify this hypothesis, further investigation into the changes in Nrf2 expression over time is required. However, as mentioned above, because the expression of several genes that are controlled by Nrf2 were changed in DMF groups, Nrf2 activation might be continued and/or increased by DMF.

Gene expression of inflammatory cytokines such as TNF-α and IL-6 tended to be suppressed by DMF, and particularly, TNF-α was significantly decreased at the highest dose in Experiment 1 (7,500 ppm). A previous study also showed that DMF inhibited the production of pro-inflammatory cytokines such as TNF-α and IL-6[36, 37]. Considering the histopathological results, DMF might have an anti-inflammatory effect on CIS-induced renal tubulointerstitial lesions.

In conclusion, DMF is suggested to reduce CIS-induced renal tubular injury via NQO1- mediated antioxidant mechanisms and reduce the consequent tubulointerstitial fibrosis as well.

Disclosure of Potential Conflicts of Interest: The authors declare that there is no conflict of interest.

References

1. Lulich JP, Osborne CA, O'Brien TD, and Polzin DJ. Feline renal failure: questions, answers, questions. Compend Contin Educ Pract Vet. **14**: 127–152. 1992.
2. Chevalier RL, Forbes MS, and Thornhill BA. Ureteral obstruction as a model of renal interstitial fibrosis and obstructive nephropathy. Kidney Int. **75**: 1145–1152. 2009. [Medline] [CrossRef]
3. Yang X, Zhang HY, Zhang YJ, Li YJ, Chen WY, and Yu XQ. [Expression of peroxisome proliferators-activated receptor gamma and alpha-smooth muscle actin in unilateral ureteral obstruction in rats]. Zhongguo Wei Zhong Bing Ji Jiu Yi Xue. **17**: 611–614. 2005. (in Chinese) [Medline]
4. Hesketh EE, Czopek A, Clay M, Borthwick G, Ferenbach D, Kluth D, and Hughes J. Renal ischaemia reperfusion injury: a mouse model of injury and regeneration. J Vis Exp. **88**: 51816. 2014. [Medline]
5. Yamate J, Ishida A, Tsujino K, Tatsumi M, Nakatsuji S, Kuwamura M, Kotani T, and Sakuma S. Immunohistochemical study of rat renal interstitial fibrosis induced by repeated injection of cisplatin, with special reference to the kinetics of macrophages and myofibroblasts. Toxicol Pathol. **24**: 199–206. 1996. [Medline] [CrossRef]
6. Yamate J, Sato K, Machida Y, Ide M, Sato S, Nakatsuji S, Kuwamura M, Kotani T, and Sakuma S. Cisplatin-induced rat renal interstitial fibrosis; a possible pathogenesis based on the data. J Toxicol Pathol. **13**: 237–247. 2000. [CrossRef]
7. Suzuki K, Uetsuka K, Nakayama H, Doi C, and Doi K. Renal tubulointerstitial lesions in mercuric chloride-treated Brown Norway rats. J Toxicol Pathol. **11**: 241–247. 1998. [CrossRef]
8. Suzuki K, Uetsuka K, Nakayama H, and Doi K. Kinetics of transforming growth factor-beta1 and extracellular matrix in renal tubulointerstitial lesions of mercuric chloride-treated Brown Norway rats. Int J Exp Pathol. **80**: 125–132. 1999. [Medline] [CrossRef]
9. Boulikas T, and Vougiouka M. Cisplatin and platinum drugs at the molecular level. (Review). Oncol Rep. **10**: 1663–1682. 2003. [Medline]
10. Okamura M, Hashimoto K, Shimada J, and Sakagami H. Apoptosis-inducing activity of cisplatin (CDDP) against human hepatoma and oral squamous cell carcinoma cell lines. Anticancer Res. **24**(2B): 655–661. 2004. [Medline]
11. Tsutsumishita Y, Onda T, Okada K, Takeda M, Endou H, Futaki S, and Niwa M. Involvement of H2O2 production in cisplatin-induced nephrotoxicity. Biochem Biophys Res Commun. **242**: 310–312. 1998. [Medline] [CrossRef]
12. Gong JG, Costanzo A, Yang HQ, Melino G, Kaelin WG Jr, Levrero M, and Wang JY. The tyrosine kinase c-Abl regulates p73 in apoptotic response to cisplatin-induced DNA damage. Nature. **399**: 806–809. 1999. [Medline] [CrossRef]
13. Mills EA, Ogrodnik MA, Plave A, and Mao-Draayer Y. Emerging understanding of the mechanism of action for dimethyl fumarate in the treatment of multiple sclerosis. Front Neurol. **9**: 5. 2018. [Medline] [CrossRef]
14. de Jong R, Bezemer AC, Zomerdijk TP, van de Pouw-Kraan T, Ottenhoff TH, and Nibbering PH. Selective stimulation of T helper 2 cytokine responses by the anti-psoriasis agent monomethylfumarate. Eur J Immunol. **26**: 2067–2074. 1996. [Medline] [CrossRef]
15. Scannevin RH, Chollate S, Jung MY, Shackett M, Patel H, Bista P, Zeng W, Ryan S, Yamamoto M, Lukashev M, and Rhodes KJ. Fumarates promote cytoprotection of central nervous system cells against oxidative stress via the nuclear factor (erythroid-derived 2)-like 2 pathway. J Pharmacol Exp Ther. **341**: 274–284. 2012. [Medline] [CrossRef]
16. Yang SM, Ka SM, Hua KF, Wu TH, Chuang YP, Lin YW, Yang FL, Wu SH, Yang SS, Lin SH, Chang JM, and Chen A. Antroquinonol mitigates an accelerated and progressive IgA nephropathy model in mice by activating the Nrf2 pathway and inhibiting T cells and NLRP3 inflammasome. Free Radic Biol Med. **61**: 285–297. 2013. [Medline] [CrossRef]
17. Wu CC, Huang YS, Chen JS, Huang CF, Su SL, Lu KC, Lin YF, Chu P, Lin SH, and Sytwu HK. Resveratrol ameliorates renal damage, increases expression of heme oxygenase-1, and has anti-complement, anti-oxidative, and anti-apoptotic effects in a murine model of membranous nephropathy. PLoS One. **10**: e0125726. 2015. [Medline] [CrossRef]
18. Qin T, Du R, Huang F, Yin S, Yang J, Qin S, and Cao W. Sinomenine activation of Nrf2 signaling prevents hyperactive inflammation and kidney injury in a mouse model of obstructive nephropathy. Free Radic Biol Med. **92**: 90–99. 2016. [Medline] [CrossRef]
19. Oh CJ, Kim JY, Choi YK, Kim HJ, Jeong JY, Bae KH, Park KG, and Lee IK. Dimethylfumarate attenuates renal fibrosis via NF-E2-related factor 2-mediated inhibition of transforming growth factor-β/Smad signaling. PLoS One. **7**: e45870. 2012. [Medline] [CrossRef]
20. Oey O, Rao P, Luciuk M, Mannix C, Rogers NM, Sagar P, Wong A, and Rangan G. Effect of dimethyl fumarate on

renal disease progression in a genetic ortholog of nephronophthisis. Exp Biol Med (Maywood). **243**: 428–436. 2018. [Medline] [CrossRef]
21. Grzegorzewska AP, Seta F, Han R, Czajka CA, Makino K, Stawski L, Isenberg JS, Browning JL, and Trojanowska M. Dimethyl Fumarate ameliorates pulmonary arterial hypertension and lung fibrosis by targeting multiple pathways. Sci Rep. **7**: 41605. 2017. [Medline] [CrossRef]
22. Zhang WX, Zhao JH, Ping FM, Liu ZJ, Gu JX, and Lu XQ. Effect of dimethyl fumarate on rats with chronic pancreatitis. Asian Pac J Trop Med. **9**: 261–264. 2016. [Medline] [CrossRef]
23. Suzuki M, Adachi K, Ogawa Y, Karasawa Y, Katsuyama K, Sugimoto T, and Doi K. The combination of fixation using PLP fixative and embedding in paraffin by the AMeX method is useful for immunohistochemical and enzyme histochemical studies of the lung. N Tox Path. **13**: 109–113. 2000. [CrossRef]
24. Livak KJ, and Schmittgen TD. Analysis of relative gene expression data using real-time quantitative PCR and the 2(-Δ Δ C(T)) Method. Methods. **25**: 402–408. 2001. [Medline] [CrossRef]
25. Nicholas JA, Boster AL, Imitola J, O'Connell C, and Racke MK. Design of oral agents for the management of multiple sclerosis: benefit and risk assessment for dimethyl fumarate. Drug Des Devel Ther. **8**: 897–908. 2014. [Medline]
26. Šilhavý J, Zídek V, Mlejnek P, Landa V, Šimáková M, Strnad H, Oliyarnyk O, Škop V, Kazdová L, Kurtz T, and Pravenec M. Fumaric acid esters can block pro-inflammatory actions of human CRP and ameliorate metabolic disturbances in transgenic spontaneously hypertensive rats. PLoS One. **9**: e101906. 2014. [Medline] [CrossRef]
27. Meng XM, Wang S, Huang XR, Yang C, Xiao J, Zhang Y, To KF, Nikolic-Paterson DJ, and Lan HY. Inflammatory macrophages can transdifferentiate into myofibroblasts during renal fibrosis. Cell Death Dis. **7**: e2495. 2016. [Medline] [CrossRef]
28. Prunotto M, Ghiggeri G, Bruschi M, Gabbiani G, Lescuyer P, Hocher B, Chaykovska L, Berrera M, and Moll S. Renal fibrosis and proteomics: current knowledge and still key open questions for proteomic investigation. J Proteomics. **74**: 1855–1870. 2011. [Medline] [CrossRef]
29. Hesketh M, Sahin KB, West ZE, and Murray RZ. Macrophage phenotypes regulate scar formation and chronic wound healing. Int J Mol Sci. **18**: 1545. 2017. [Medline] [CrossRef]
30. Suzuki K, Kanabayashi T, Nakayama H, and Doi K. Kinetics of chemokines and their receptors in mercuric chloride-induced tubulointerstitial lesions in brown Norway rats. Exp Mol Pathol. **75**: 58–67. 2003. [Medline] [CrossRef]
31. Gang GT, Kim YH, Noh JR, Kim KS, Jung JY, Shong M, Hwang JH, and Lee CH. Protective role of NAD(P)H:quinone oxidoreductase 1 (NQO1) in cisplatin-induced nephrotoxicity. Toxicol Lett. **221**: 165–175. 2013. [Medline] [CrossRef]
32. Chen X, Wei SY, Li JS, Zhang QF, Wang YX, Zhao SL, Yu J, Wang C, Qin Y, Wei QJ, Lv GX, and Li B. Overexpression of heme oxygenase-1 prevents renal interstitial inflammation and fibrosis induced by unilateral ureter obstruction. PLoS One. **11**: e0147084. 2016. [Medline] [CrossRef]
33. Gopal S, Mikulskis A, Gold R, Fox RJ, Dawson KT, and Amaravadi L. Evidence of activation of the Nrf2 pathway in multiple sclerosis patients treated with delayed-release dimethyl fumarate in the Phase 3 DEFINE and CONFIRM studies. Mult Scler. **23**: 1875–1883. 2017. [Medline] [CrossRef]
34. Mitsuishi Y, Taguchi K, Kawatani Y, Shibata T, Nukiwa T, Aburatani H, Yamamoto M, and Motohashi H. Nrf2 redirects glucose and glutamine into anabolic pathways in metabolic reprogramming. Cancer Cell. **22**: 66–79. 2012. [Medline] [CrossRef]
35. Stanton RC. Glucose-6-phosphate dehydrogenase, NADPH, and cell survival. IUBMB Life. **64**: 362–369. 2012. [Medline] [CrossRef]
36. Smith MD, Martin KA, Calabresi PA, and Bhargava P. Dimethyl fumarate alters B-cell memory and cytokine production in MS patients. Ann Clin Transl Neurol. **4**: 351–355. 2017. [Medline] [CrossRef]
37. Li R, Rezk A, Ghadiri M, Luessi F, Zipp F, Li H, Giacomini PS, Antel J, and Bar-Or A. Dimethyl fumarate treatment mediates an anti-inflammatory shift in B cell subsets of patients with multiple sclerosis. J Immunol. **198**: 691–698. 2017. [Medline] [CrossRef]